NASA/TM—2005-213436

Crystallization Kinetics of a Solid Oxide Fuel Cell Seal Glass by Differential Thermal Analysis

Narottam P. Bansal and Eleanor A. Gamble
Glenn Research Center, Cleveland, Ohio

January 2005

The NASA STI Program Office . . . in Profile

Since its founding, NASA has been dedicated to the advancement of aeronautics and space science. The NASA Scientific and Technical Information (STI) Program Office plays a key part in helping NASA maintain this important role.

The NASA STI Program Office is operated by Langley Research Center, the Lead Center for NASA's scientific and technical information. The NASA STI Program Office provides access to the NASA STI Database, the largest collection of aeronautical and space science STI in the world. The Program Office is also NASA's institutional mechanism for disseminating the results of its research and development activities. These results are published by NASA in the NASA STI Report Series, which includes the following report types:

- TECHNICAL PUBLICATION. Reports of completed research or a major significant phase of research that present the results of NASA programs and include extensive data or theoretical analysis. Includes compilations of significant scientific and technical data and information deemed to be of continuing reference value. NASA's counterpart of peer-reviewed formal professional papers but has less stringent limitations on manuscript length and extent of graphic presentations.

- TECHNICAL MEMORANDUM. Scientific and technical findings that are preliminary or of specialized interest, e.g., quick release reports, working papers, and bibliographies that contain minimal annotation. Does not contain extensive analysis.

- CONTRACTOR REPORT. Scientific and technical findings by NASA-sponsored contractors and grantees.

- CONFERENCE PUBLICATION. Collected papers from scientific and technical conferences, symposia, seminars, or other meetings sponsored or cosponsored by NASA.

- SPECIAL PUBLICATION. Scientific, technical, or historical information from NASA programs, projects, and missions, often concerned with subjects having substantial public interest.

- TECHNICAL TRANSLATION. English-language translations of foreign scientific and technical material pertinent to NASA's mission.

Specialized services that complement the STI Program Office's diverse offerings include creating custom thesauri, building customized databases, organizing and publishing research results . . . even providing videos.

For more information about the NASA STI Program Office, see the following:

- Access the NASA STI Program Home Page at ***http://www.sti.nasa.gov***

- E-mail your question via the Internet to help@sti.nasa.gov

- Fax your question to the NASA Access Help Desk at 301–621–0134

- Telephone the NASA Access Help Desk at 301–621–0390

- Write to:
  NASA Access Help Desk
  NASA Center for AeroSpace Information
  7121 Standard Drive
  Hanover, MD 21076

NASA/TM—2005-213436

Crystallization Kinetics of a Solid Oxide Fuel Cell Seal Glass by Differential Thermal Analysis

Narottam P. Bansal and Eleanor A. Gamble
Glenn Research Center, Cleveland, Ohio

Prepared for the
Ninth International Symposium on Solid Oxide Fuel Cells (SOFC–IX)
cosponsored by the Electrochemical Society and the SOFC Society of Japan
Quebec City, Canada, May 15–20, 2005

National Aeronautics and
Space Administration

Glenn Research Center

January 2005

Acknowledgments

Thanks are due to John Setlock for technical assistance during this work, Anna Palczer for DTA analysis, and Ralph Garlick for X-ray diffraction measurements. Eleanor Gamble was a student intern from Purdue University at NASA Glenn during the summer of 2003.

This work was sponsored by the Low Emissions Alternative Power Project of the Vehicle Systems Program at the NASA Glenn Research Center.

Available from

NASA Center for Aerospace Information
7121 Standard Drive
Hanover, MD 21076

National Technical Information Service
5285 Port Royal Road
Springfield, VA 22100

Available electronically at http://gltrs.grc.nasa.gov

Crystallization Kinetics of a Solid Oxide Fuel Cell Seal Glass by Differential Thermal Analysis

Narottam P. Bansal and Eleanor A. Gamble
National Aeronautics and Space Administration
Glenn Research Center
Cleveland, Ohio 44135

Abstract

Crystallization kinetics of a barium calcium aluminosilicate glass (BCAS), a sealant material for planar solid oxide fuel cells, have been investigated by differential thermal analysis (DTA). From variation of DTA peak maximum temperature with heating rate, the activation energy for glass crystallization was calculated to be 259 kJ/mol. Development of crystalline phases on thermal treatments of the glass at various temperatures has been followed by powder x-ray diffraction. Microstructure and chemical composition of the crystalline phases were investigated by scanning electron microscopy and energy dispersive spectroscopic (EDS) analysis. $BaSiO_3$ and hexacelsian ($BaAl_2Si_2O_8$) were the primary crystalline phases whereas monoclinic celsian ($BaAl_2Si_2O_8$) and (Ba_x, Ca_y)SiO_4 were also detected as minor phases. Needle-shaped $BaSiO_3$ crystals are formed first, followed by the formation of other phases at longer times of heat treatments. The glass does not fully crystallize even after long term heat treatments at 750 to 900 °C.

1. Introduction

Solid oxide fuel cells (SOFCs) (ref. 1) are being developed for a broad range of applications including portable electronic devices, automobiles, power generation, aeronautics, etc. The salient features of SOFC are all solid construction and high-temperature electrochemical reaction based operation, resulting in clean and efficient power generation from a variety of fuels. SOFCs of two different designs, tubular and planar, are currently under development. Planar SOFCs offer several advantages such as simple manufacturing and relatively short current path resulting in higher power density and efficiency. However, planar SOFCs require hermetic seals to separate and contain fuel and oxidant within the cell and to bond cell components together. The requirements for SOFC sealing materials are severe since the cells will operate at 600 to 1000 °C for thousands of hours, with sealing materials exposed to both oxidizing and reducing conditions. The seals must be chemically and mechanically compatible with different oxide and metallic cell components and should be electrically insulating. Also, they must survive cycling between room and operational temperatures. Various glass and glass-ceramics based on borates, phosphates and silicates are being examined (refs. 2 to 8) for SOFC seals. Silicate glasses are expected to perform superior to the borate and phosphate glasses. A barium calcium aluminosilicate (BCAS) glass composition appears to be quite promising (ref. 2). Chemical compatibility of this BCAS glass with metallic interconnects has been investigated (refs. 9 and 10).

The main objective of the present work was to investigate the crystallization kinetics of the BCAS glass. Another objective was to study the formation of crystalline phase(s) in the glass under conditions which are similar to those at which the solid oxide fuel cell is sealed and operated.

2. Experimental Methods

A barium calcium aluminosilicate (BCAS) glass of composition (mol %) 35BaO-15CaO-5Al_2O_3-10B_2O_3-35SiO_2 was obtained in the form of powder and frit from a commercial vendor. The glass powder had an average particle size of 14.2 μm.

Crystallization kinetics of the BCAS glass were studied by differential thermal analysis (DTA) using a Netzsch STA 409C system interfaced with a computerized data acquisition and analysis system. Glass samples were contained in alumina cups. DTA scans were recorded from room temperature to 1000 to 1100 °C in flowing dry argon at various heating rates of 2 to 40 °C/min. Glass transition temperatures (T_g) and crystallization peak maximum temperatures (T_p) were obtained from the DTA scans.

The development of crystalline phases in the BCAS glass was investigated by isothermal heat treatments of bulk and powder samples in an electric furnace in air. The samples were heat treated for 1 to 100 h at various temperatures from 700 to 1000 °C. Phases crystallizing in the heat treated glasses were identified from powder x-ray diffraction (XRD) patterns recorded at room temperature using a step scan procedure (0.03°/2θ step, count time 0.4 s) on a Philips ADP-3600 automated diffractometer equipped with a crystal monochromator employing Copper K_α radiation.

Microstructures of the polished cross-sections of heat treated glass specimens were observed using a JEOL JSM-840A scanning electron microscope (SEM). Prior to analysis, a thin layer of Pt or carbon was evaporated onto the SEM specimens for electrical conductivity. Qualitative x-ray elemental analysis of various phases was carried out using a Kevex Delta thin window energy dispersive spectrometer (EDS) and analyzer.

3. Theoretical Background

The kinetics of phase transformation, such as crystallization of a glass, at a constant temperature can be described by the Johnson-Mehl-Avrami (JMA) equation (refs. 11 and 12):

$$-\ln(1 - x) = (kt)^n \tag{1}$$

where x is the volume fraction of the glass crystallized after time t, n is the dimensionless Avrami exponent which is related to the morphology of crystal growth, and k is the reaction rate constant. The temperature dependence of k (at least within narrow temperature ranges) can be expressed by the Arrhenius equation:

$$k = \upsilon \exp[-E/RT] \tag{2}$$

where E is the effective overall activation energy for the transformation process, υ is an effective frequency factor which is a measure of the probability that a molecule having energy E participates in the transformation, R is the gas constant, and T is the absolute reaction temperature.

During a non-isothermal DSC or DTA scan, the sample temperature changes linearly with time at a rate θ (= dT/dt):

$$T = T_i + \theta t \tag{3}$$

where T_i is the initial temperature. In eq. (1) the right-hand side corresponds to growth in volume of crystal nuclei. However, for the non-isothermal case the rate constant changes continuously with time due to the changing temperature, so that the JMA relation must be written as:

$$-\ln(1-x) = \left(\int_0^t k(t)dt\right)^n \tag{4}$$

If at each temperature, the deflection of the DSC or DTA trace from its baseline is proportional to the instantaneous crystallization rate (Borchard assumption (ref. 13)), then the rate of sample transformation is maximum at the peak of the crystallization exotherm. Bansal et al. (refs. 14 to 16) have earlier shown that the temperature T_p of the crystallization peak changes with heating rate θ according to the relation:

$$\ln(T_p^2/\theta) = \ln(E/R\upsilon) + E/RT_p \tag{5}$$

Hence a plot of $\ln(T_p^2/\theta)$ versus $1/T_p$ should be linear with a slope of E/R and an intercept $[\ln(E/R) - \ln \upsilon]$. Equation (5) is based on the assumption that at the temperature corresponding to the maximum in the crystallization exothermic peak, the degree of crystallization attains the same specific value independent of the heating rate. Earlier studies have shown that the crystallization kinetic parameters obtained by isothermal and non-isothermal DSC using eq. (5) are in good agreement, particularly when both studies are carried out in the same temperature range.

Values of the Avrami parameter n can be evaluated from the non-isothermal data using an expression derived by Piloyan et al. (ref. 17) which is valid in the range $0 < x < 0.2$:

$$d\ln(\Delta y)/d(1/T) = -nE/R \tag{6}$$

where (Δy) is the vertical displacement at temperature T of the DSC or DTA crystallization exotherm from the baseline. The Avrami parameter n gives an indication of the crystal growth mechanism in the glass.

4. Experimental Results

4.1. Physical Properties of Glass

Chemical composition of the BCAS glass and some of its physical, thermal and mechanical properties are listed in table I. The T_g value of 619 °C for this glass is below the SOFC operating temperature. The coefficient of thermal expansion (CTE) of this glass (10.5 – 11.8 x 10^{-6} /°C) is in the same range as the CTE of other SOFC components: cathode, anode, electrolyte, and interconnect.

TABLE I.—PROPERTIES OF BCAS GLASS

Property	Value
Composition	35BaO-15CaO-5Al_2O_3-10B_2O_3-35SiO_2 (mol %) 56.4BaO-8.8CaO-5.4Al_2O_3-7.3B_2O_3-22.1SiO_2 (wt %)
Average particle size	14.2 μm
Density	3.88 g/cm^3
Glass transition temp.	619 °C
Dilatometric softening point	682 °C
Coefficient of thermal expansion	10.5 x 10^{-6} /°C (RT –500 °C); 11.8 x 10^{-6} /°C (20 to 800 °C)
Young's modulus	72 GPa
Microhardness	5.96 GPa
Flexure strength	50 MPa
Fracture toughness	0.56 MPa.$m^{1/2}$

4.2. Crystallization Kinetics by DTA

DTA scans for BCAS glass were recorded at various heating rates from 2 to 40 °C/min. Typical scans at heating rates of 10 and 40 °C/min are shown in figure 1 (a) and (b), respectively. The first endothermic peak at ~650 to 680 °C is due to the glass transition and the broad exothermic peak is due to crystallization of the glass. The second endothermic peak at ~940 to 1000 °C is from the melting of crystalline phases and residual glass. Influence of scan rate on crystallization peak temperature (T_p) is given in table II.

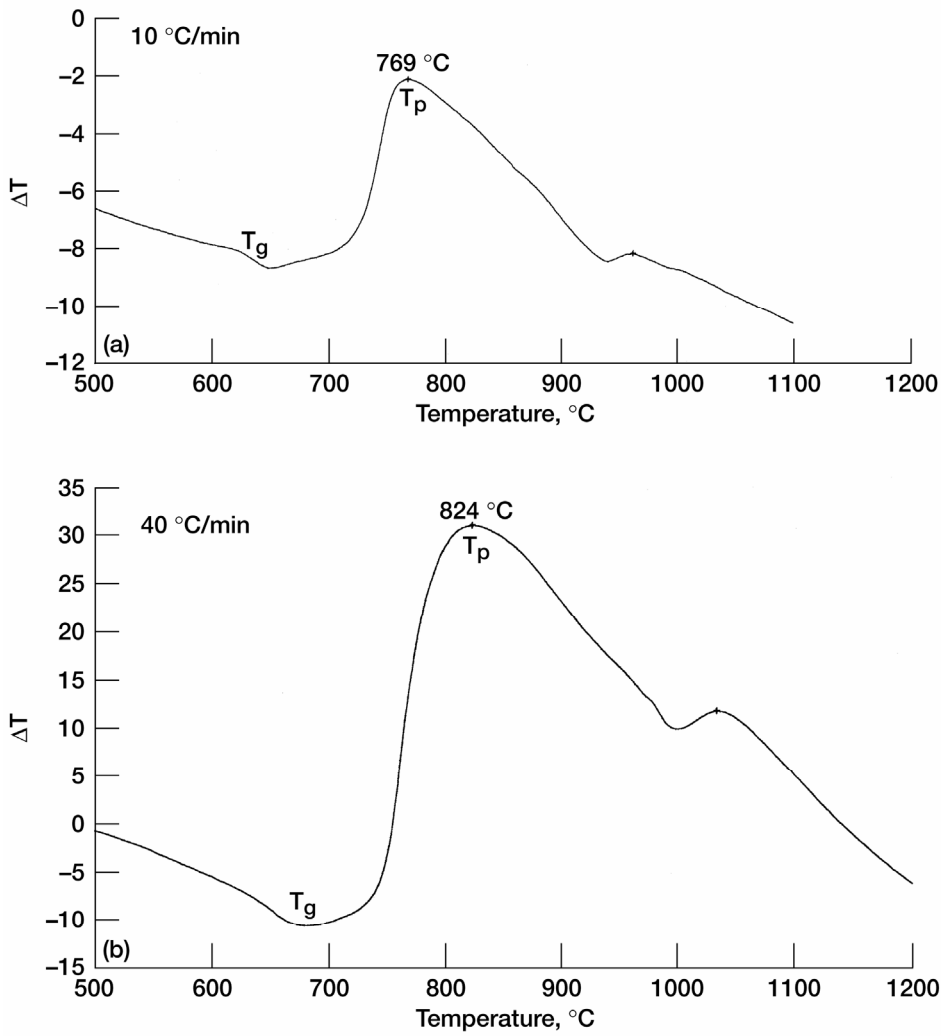

Figure 1.—DTA thermograms of BCAS glass.

TABLE II.—EFFECT OF HEATING RATE ON DTA CRYSTALLIZATION PEAK TEMPERATURES (T_p) OF BCAS GLASS

Scan rate (°C/min)	T_p (°C)
2	726.9
5	749.3
10	769.0
20	785.7
30	814.2
40	823.6

4.3. Crystal Phase Development by X-ray Diffraction

The results of crystal phase development in BCAS glass after heat treatments at various temperatures between 700 to 1000 °C for different times are summarized in table III. $BaSiO_3$ is the first phase to crystallize out in this glass. This is followed by the formation of hexacelsian $BaAl_2Si_2O_8$. The $BaSiO_3$ and hexacelsian were the primary crystalline phases whereas monoclinic celsian ($BaAl_2Si_2O_8$) and $(Ba_xCa_y)SiO_4$ were also detected as minor phases. Needle-shaped $BaSiO_3$ crystals are formed first followed by the formation of other phases at longer times of heat treatments. Crystallization occurred most rapidly at 800 °C. After 1000 °C heat treatment, all samples were totally amorphous.

TABLE III.—CRYSTALLINE PHASE DEVELOPMENT IN BCAS GLASS ON HEAT TREATMENTS

Heat treatment		Crystalline phases detected from x-ray diffraction					
Temp. (°C)	Time (h)	Amorphous	$BaSiO_3$	Hexacelsian	Celsian	$(Ba_{1.5}Ca_{0.5})SiO_4$	$(Ba_{1.31}Ca_{0.69})SiO_4$
700	20	X					
	50	X	X				
750	3	X					
	5	X	X				
	10	X	X				
	100	X	X	X	X		
800	1	X	X				
	5	X	X	X			
	18	X	X	X		X	
	50	X	X	X		X	
	100	X	X	X			
850	21	X	X	X			
	100	X	X		X		X
900	10	X	X	X			
	100	X	X	X			
1000	10	X					
	50	X					

4.4. Microstructure

Figure 2 shows the SEM micrographs at various magnifications taken from a glass specimen heat treated for 5 hr at 800 °C. Backscatter SEM micrographs taken from polished cross-sections of glass specimens heat treated at 800 °C for different times are shown in figure 3. Barium silicate is first seen as white long elongated crystals growing in the amorphous material in the sample heated for 1 hour. After five hours, hexacelsian becomes visible as darker needle shaped crystals in the amorphous material. The dark round regions are alumina. Gray smooth areas are the residual amorphous glass phase consisting of barium-calcium aluminosilicate. The chemical compositions of various phases were confirmed using EDS analysis. The micrographs of samples heat treated for 10 and 40 hours show the crystals of various phases growing and impinging on each other. SEM micrographs of glass samples heat treated for 100 hr at 750, 800 and 850 °C are presented in figures 4, 5, and 6 respectively.

SEM micrograph and x-ray dot maps of various elements from the polished cross-section of BCAS glass heat treated at 800 °C for 1 hr is shown in figure 7. A number of phases are present. Bright elongated dendrite shaped crystals consist of $BaSiO_3$. The dark region in the middle is identified as Al_2O_3.

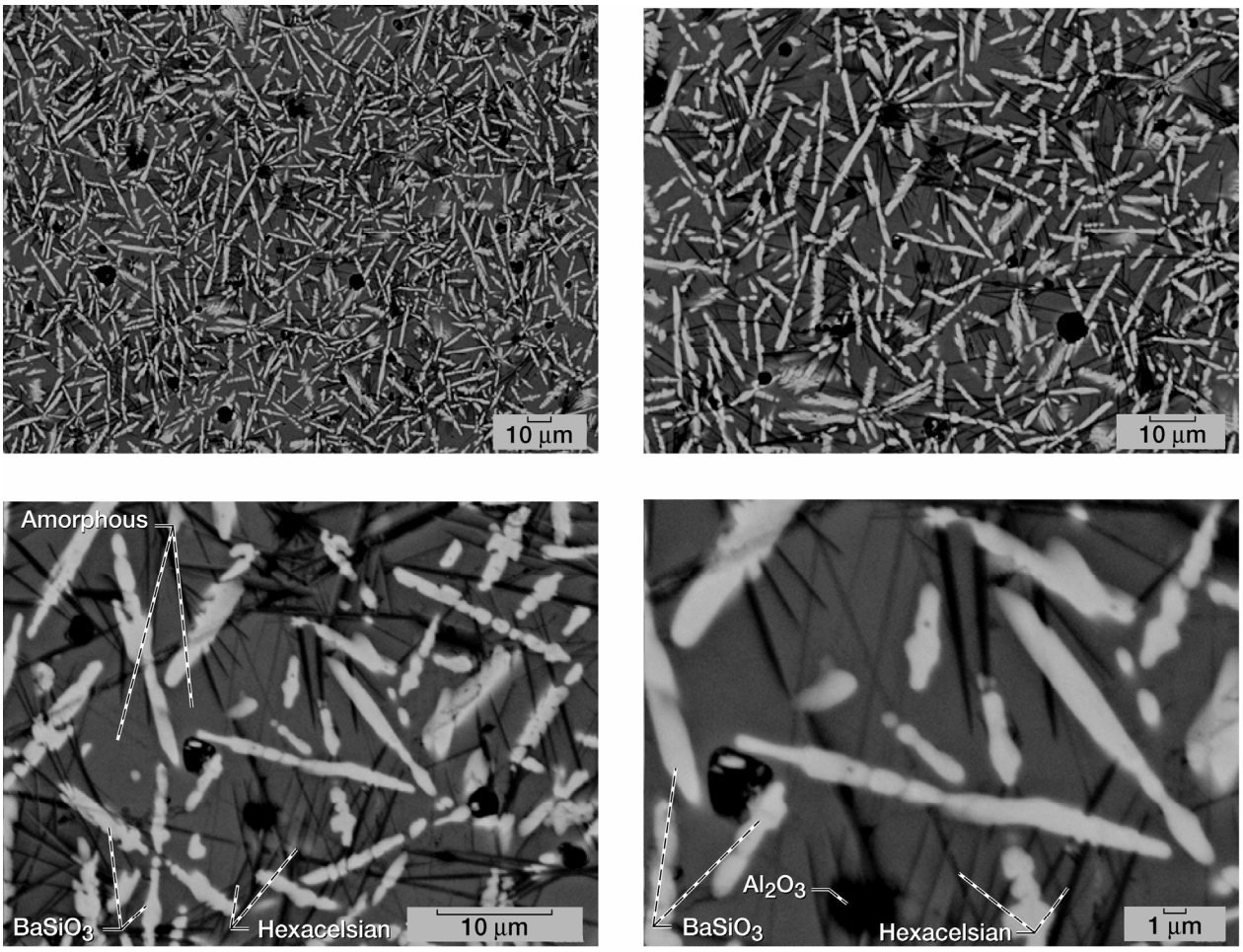

Figure 2.—SEM backscatter micrographs of polished cross-sections of BCAS glass heat-treated at 800 ˚C for 5 h.

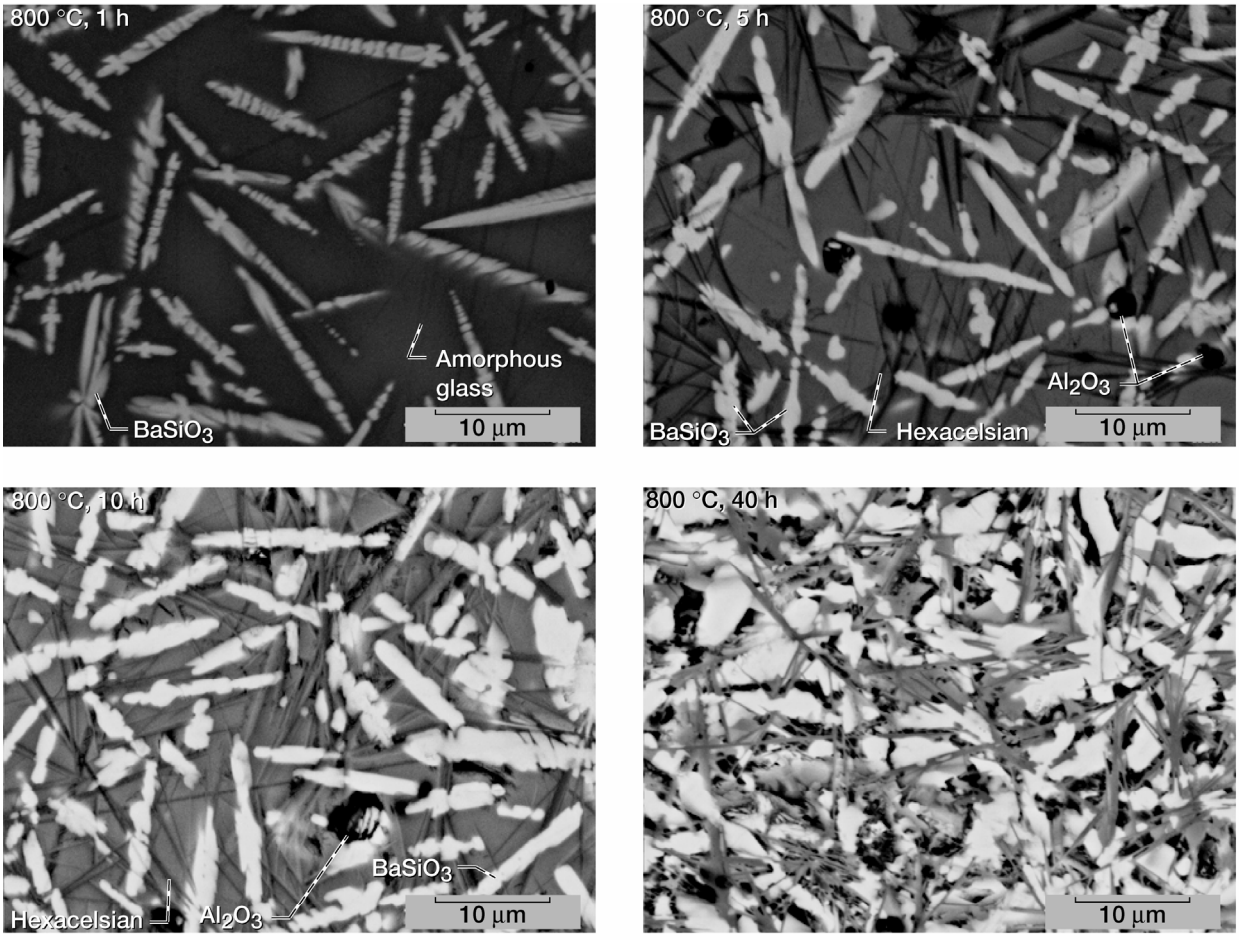

Figure 3.—SEM backscatter micrographs of polished cross-sections of BCAS glass heat-treated at 800 °C for various times.

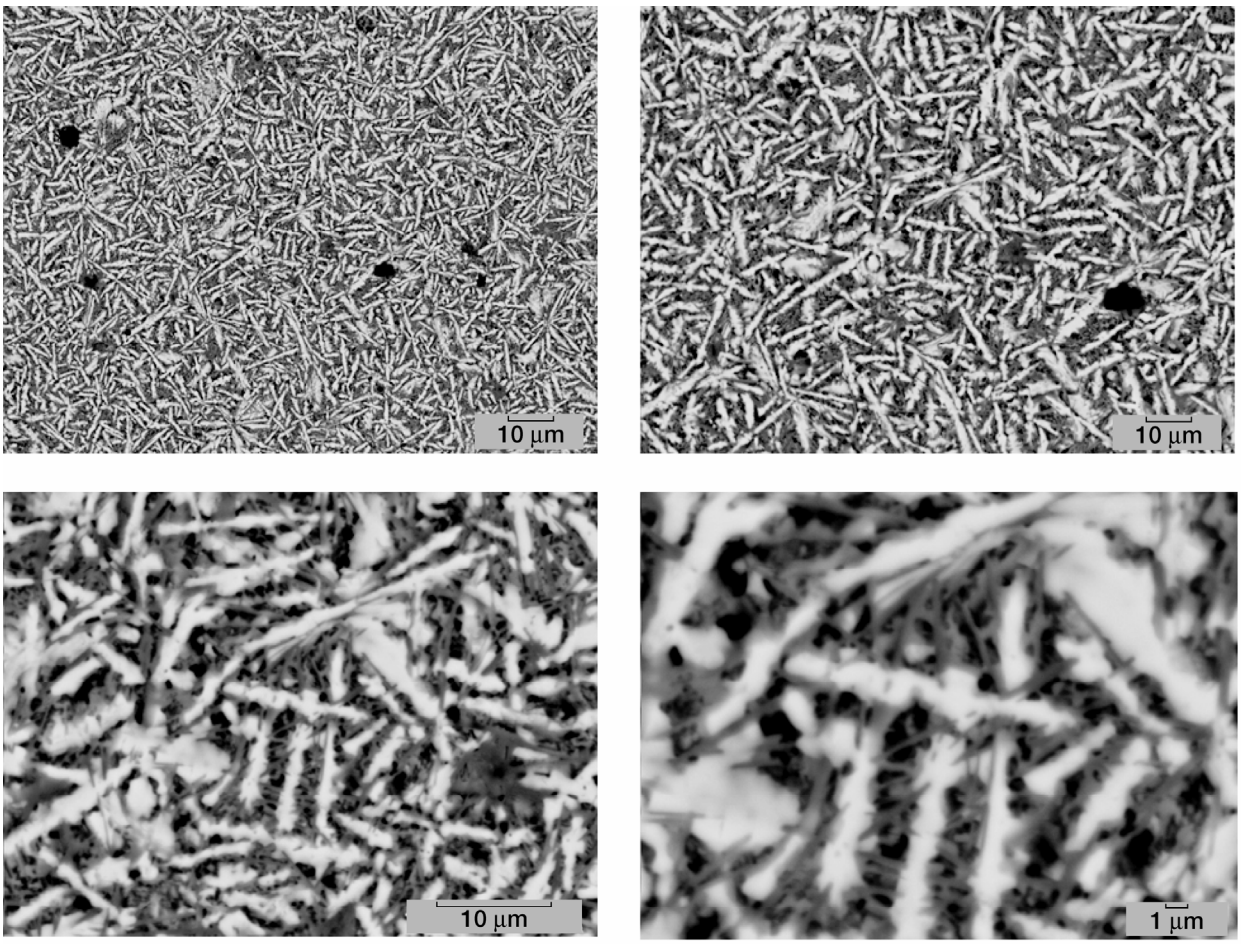

Figure 4.—SEM backscatter micrographs of polished cross-section of BCAS glass heat-treated at 750 °C for 100 h.

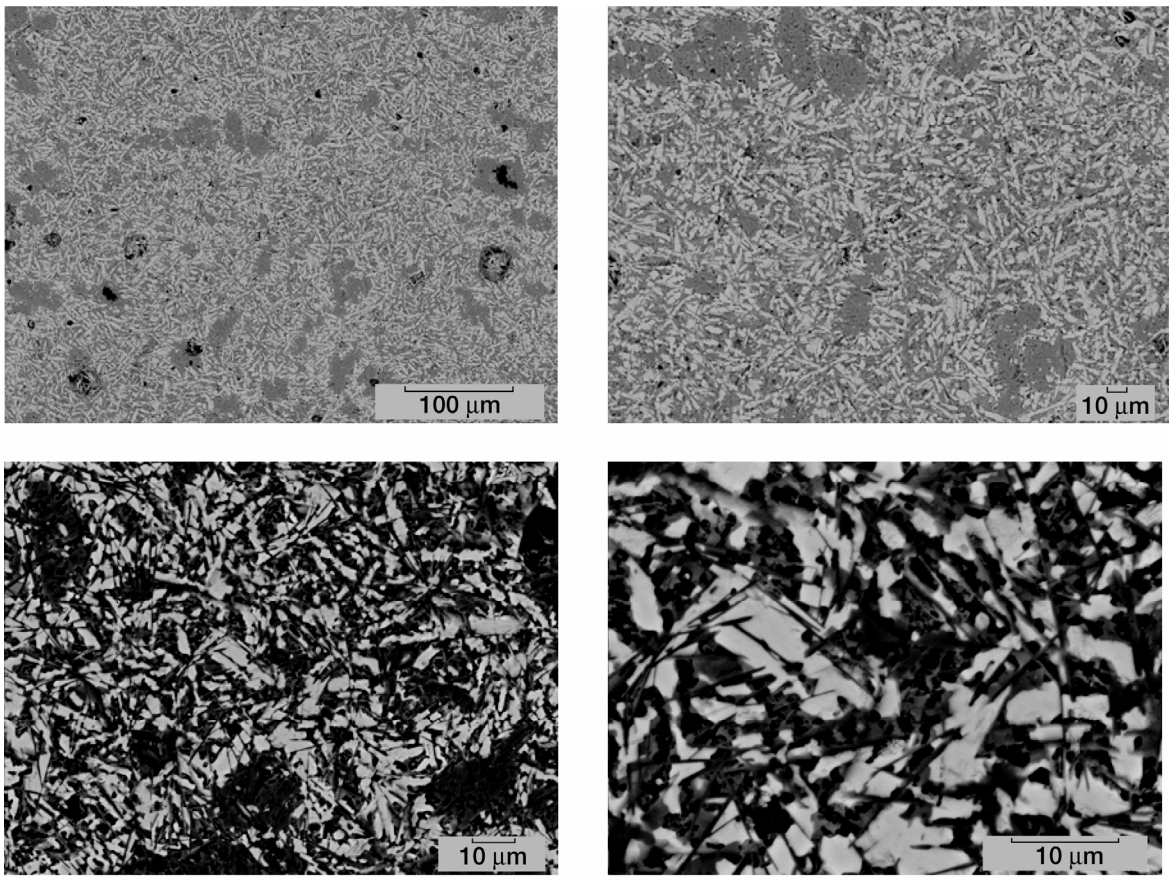

Figure 5.—SEM backscatter micrographs of polished cross-section of BCAS glass heat-treated at 800 °C for 100 h.

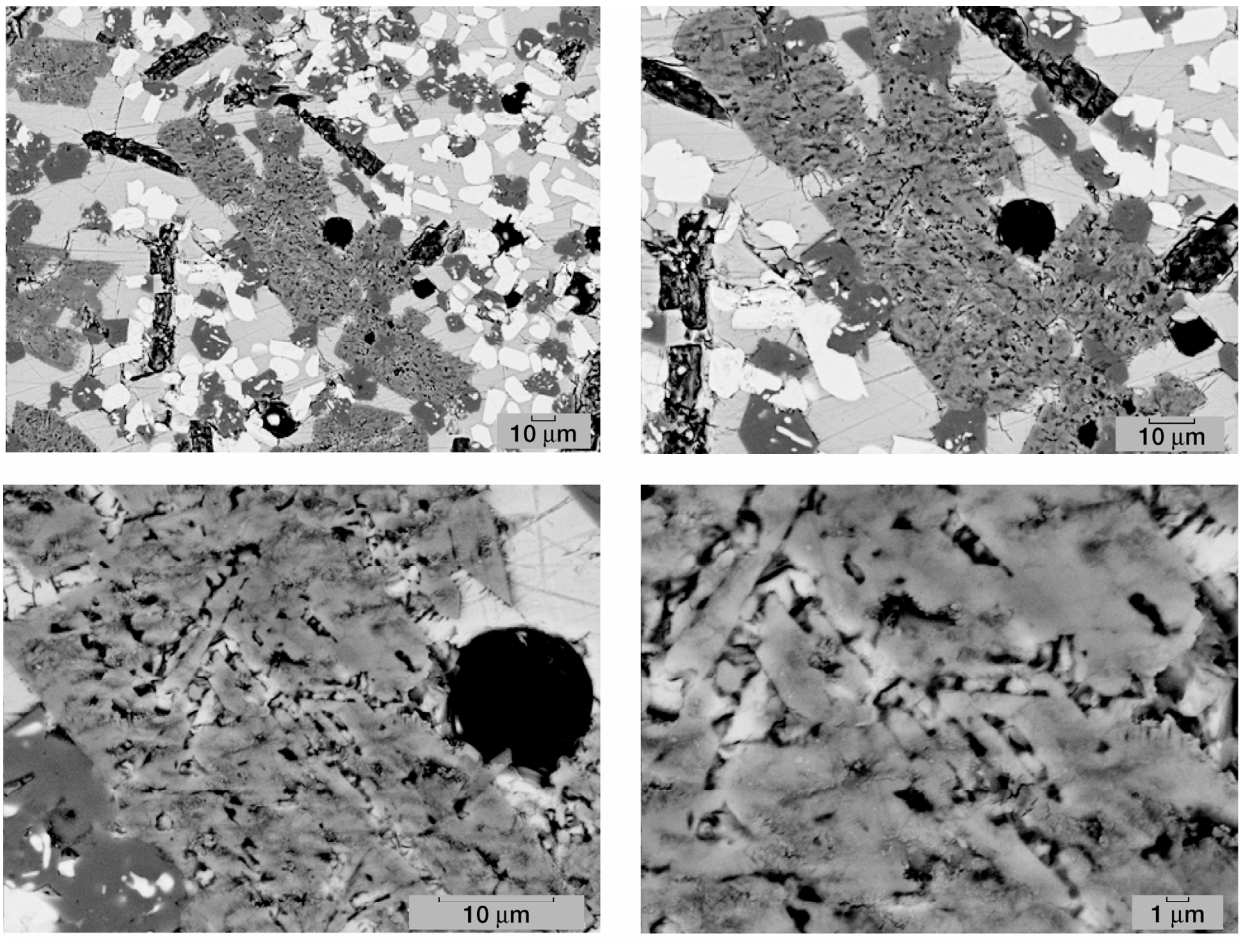

Figure 6.—SEM backscatter micrographs of polished cross-section of BCAS glass heat-treated at 850 ˚C for 100 h.

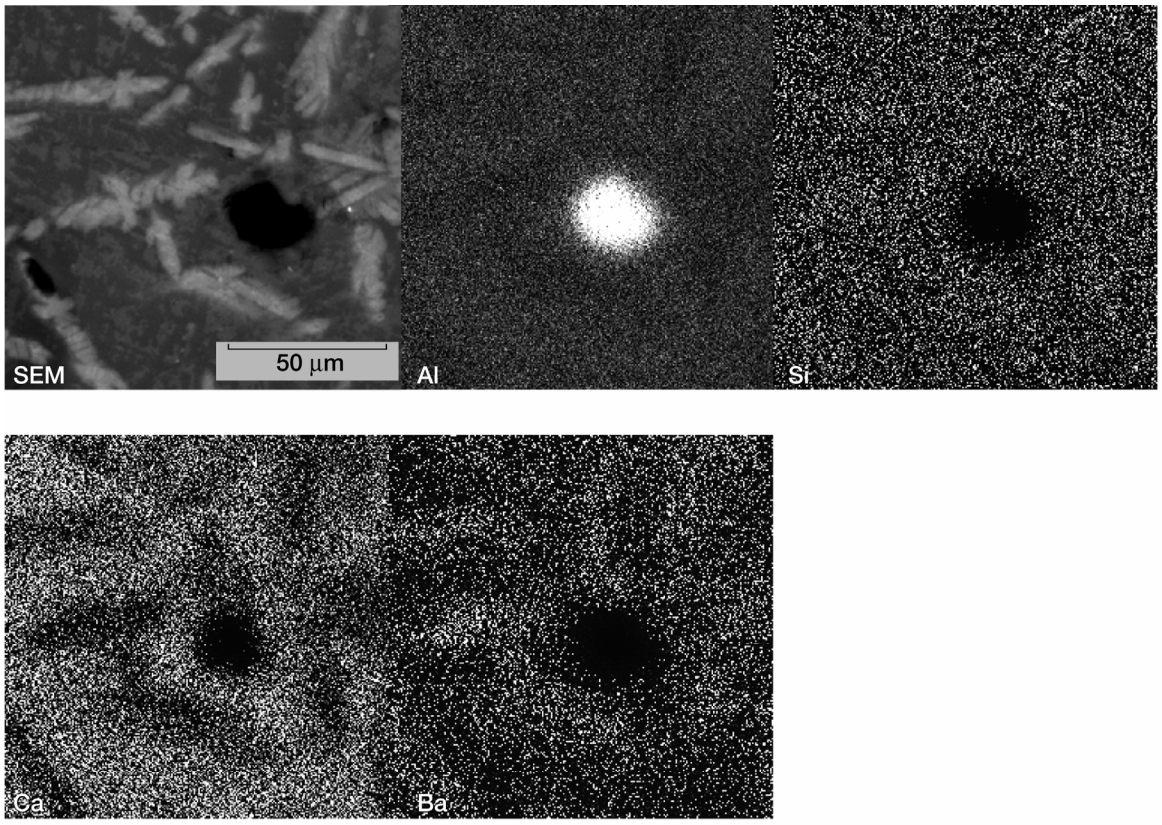

Figure 7.—SEM micrograph and x-ray dot maps of various elements from polished cross-section of BCAS glass heat-treated at 800 °C for 1h.

5. Discussion

The crystallization peak maximum temperature is seen to increase with increase in heating rate (table II). The crystallization peak maximum in the DTA or DSC scans corresponds to the temperature at which the rate of transformation of the viscous liquid into crystals becomes maximum. When the crystalline phase has the same composition as the liquid, the transformation rate will depend on the density of crystallization sites. However, when the composition of the crystalline phase is different from that of the liquid, as in the present case, the rate of transformation will be controlled by the rate of diffusion through the viscous liquid and the number of crystallization sites to which diffusion can occur. If the number of nucleation sites is increased, e.g., by using slower heating rates, the peak maximum will occur at a temperature at which the melt viscosity is higher, i.e., at a lower temperature. This explains the increase in T_p with the heating rate (table II) observed in the present study.

Plot of $\ln(T_p^2/\theta)$ versus $1/T_p$ for crystallization of the glass is shown in figure 8. A linear plot indicates validity of the kinetic model of Bansal et al. (refs. 14 to 16) and validity of the assumptions made in this model. Values of kinetic parameters E and υ obtained from linear least squares fitting of the experimental data are listed in table IV. The crystallization activation energy of 259 kJ/mol for BCAS glass is much lower than 473 to 560 kJ/mol, reported earlier for barium aluminosilicate (BAS) and strontium aluminosilicate (SAS) glasses (refs. 18 to 19) as well as 420 kJ/mol for magnesium aluminosilicate (MAS) glass (ref. 20). The Piloyan plot of $\ln(\Delta y)$ versus $1/T$ for crystallization of BCAS glass (fig. 9) is linear. Deviations were observed at higher temperatures as the Piloyan's equation is valid only in the range $0 < x < 0.2$. The value of n obtained from least squares fitting of linear part of the data to eq. (6) was 2.6. The value of n depends on the mechanism of the transformation reaction. Possible values

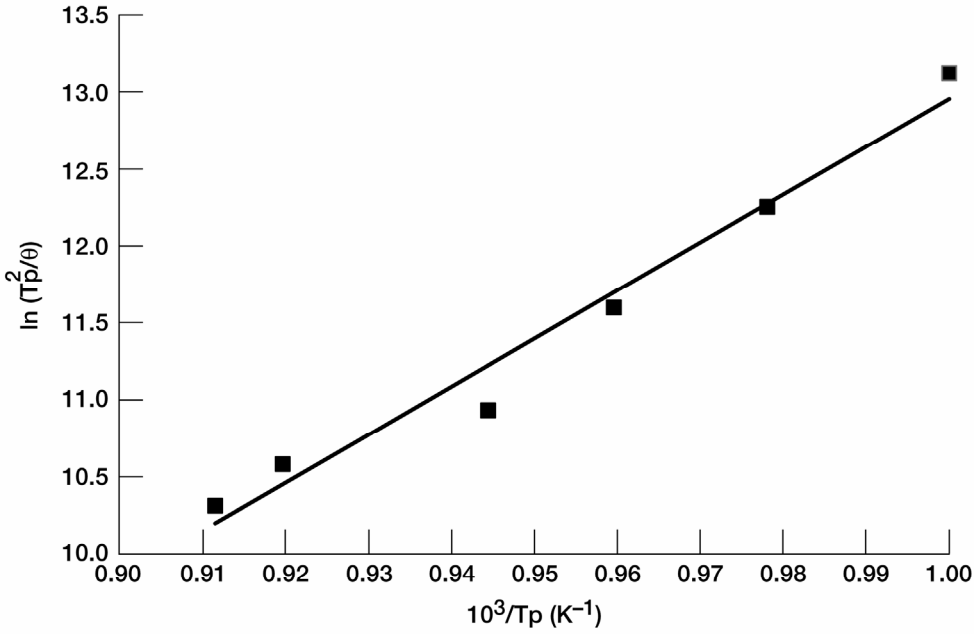

Figure 8.—Plot of ln (Tp^2/θ) versus reciprocal of crystallization peak temperature for BCAS glass.

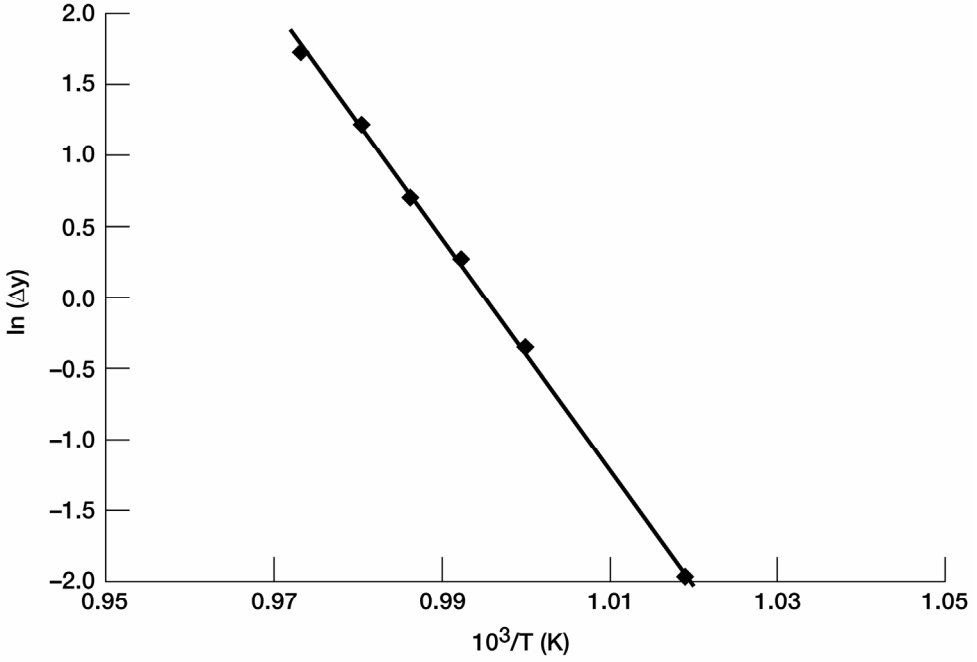

Figure 9.—Piloyan plot for the crystallization of BCAS glass for DTA thermogram recorded at scan rate of 20 K/min.

TABLE IV.—CRYSTALLIZATION KINETIC PARAMETERS FOR BCAS GLASS DETERMINED BY DTA

Parameter	Value
Activation energy, E	259 kJ/mol
Frequency factor, υ	2.6×10^{12} s^{-1}
Avrami parameter, n	2.6

of n for various mechanisms based on zero or constant nucleation rate are given in table V. If the rate of nucleation is a function of time, so is n; n is higher for a constant nucleation rate than when the nucleation rate increases with time and lies between those for constant and zero nucleation rates when the nucleation rate decreases with time. The n value of 2.6 in the present study probably corresponds to the two-dimensional growth of $BaSiO_3$ as XRD results indicated that this phase is formed first on heat treatment of BCAS glass. This is further supported by the SEM micrographs in figures 2 to 4 which show two dimensional growth of needle-shaped crystals of $BaSiO_3$ on heat treatment of the glass.

TABLE V.—POSSIBLE VALUES OF N FOR VARIOUS MECHANISMS (refs. 16 and 17)

Constant nucleation rate		Growth of constant number of nuclei (zero nucleation rate)	
Reaction mechanism	n	Reaction mechanism	n
One-dimensional growth	2	One-dimensional growth	1
Two-dimensional growth	3	Two-dimensional growth	2
Three-dimensional growth	4	Three-dimensional growth	3

The $BaSiO_3$ phase crystallizes most readily in BCAS glass. On further heat treatment, hexagonal and monoclinic $BaAl_2Si_2O_8$ and various barium-calcium silicates ($(Ba_xCa_y)SiO_4$) phases also crystallize out. Rate of crystallization depends on the heat treatment temperature.

6. Summary

Crystallization kinetics of BCAS glass have been studied by DTA. Crystallization activation energy was determined to be 259 kJ/mol. Development of crystalline phases in the glass, after isothermal heat treatments at various temperatures for different times has been investigated by x-ray diffraction and microstructural characterization. On heat treatment at 700 °C, $BaSiO_3$ crystallizes first from the glass. This is followed by the formation of hexagonal and monoclinic $BaAl_2Si_2O_8$ and barium-calcium silicate ($(Ba_xCa_y)SiO_4$) phases when treated at higher temperatures and/or longer times. After 1000 °C heat treatment, the samples were totally amorphous.

7. Conclusions

Properties of the barium calcium aluminosilicate glass of this study are compatible with those of the solid oxide fuel cell (SOFC) components such as cathode, anode, electrolyte, and interconnects. This glass does not fully crystallize even after long term heat treatments at 750 to 900 °C, the operating temperature for SOFC. Devitrification of the glass seal over a long period of time during operation of the SOFC would generate thermal stresses in the seal and may have adverse effects on its mechanical performance. This may lead to cracking of the seal, resulting in mixing of the fuel and the oxidant gases.

References

1. N.Q. Minh, Ceramic Fuel Cells, *J. Am. Ceram. Soc*., 76 [3], 563–588 (1993).
2. K.D. Meinhardt, J.D. Vienna, T.R. Armstrong, and L.R. Pederson, Glass-Ceramic Joint and Method of Joining, U.S. Patent 6,532,769, March 18, 2003.
3. K.L. Ley, M. Krumpelt, R. Kumar, J.H. Meiser, and I. Bloom, Glass-Ceramic Sealants for Solid Oxide Fuel Cells: Part I. Physical Properties, *J. Mater. Res*., 11 [6], 1489–1493 (1996).
4. S.-B. Sohn, S.-Y. Choi, G.-H. Kim, H.-S. Song, and G.-D. Kim, Suitable Glass-Ceramic Sealant for Planar Solid Oxide Fuel Cells, *J. Am. Ceram. Soc.*, 87 [2], 254–260 (2004).
5. R.E. Loehman, H.P. Dumm, and H. Hofer, Evaluation of Sealing Glasses for Solid Oxide Fuel Cells, *Ceram. Eng. Sci. Proc*., 23 [3], 699-710 (2002).
6. K. Eichler, G. Solow, P. Otschik, and W. Schaffrath, BAS ($BaO.Al_2O_3.SiO_2$) Glasses for High Temperature Applications, *J. Eur. Ceram. Soc*., 19, 1101–1104 (1999).
7. P. Geasee, R. Conradt, T. Schwickert, A. Janke, J. Remmel, and F. Tietz, Investigation of Glasses from the System $BaO\text{-}CaO\text{-}Al_2O_3\text{-}SiO_2$ Used as Sealants for the SOFC, *Proc. Int. Congr. Glass, Extended Abstracts*, 2, 47–48 (2001).
8. R. Zheng, S. R. Wang, H. W. Nie, and T.-L. Wen, $SiO_2\text{-}CaO\text{-}B_2O_3\text{-}Al_2O_3$ Ceramic Glaze as Sealant for Planar ITSOFC, *J. Power Sources*, 128[2], 165-172 (2004).
9. Z. Yang, K.D. Meinhardt, and J.W. Stevenson, Chemical Compatibility of Barium-Calcium-Aluminosilicate Based Sealing Glasses with the Ferrite Stainless Steel Interconnect in SOFCs, *J. Electrochem. Soc*., 150 [8], A1095-A1101 (2003).
10. Z. Yang, J.W. Stevenson, and K.D. Meinhardt, Chemical Interactions of Barium-Calcium-Aluminosilicate Based Sealing Glasses with Oxidation Resistant Alloys, *Solid St. Ionics*, 160[3–4], 213–225 (2003).
11. W.A. Johnson and R.F. Mehl, Reaction Kinetics in Processes of Nucleation and Growth, *Trans. Am. Inst. Elec. Eng*., 135, 416–458 (1939).
12. M. Avrami, Kinetics of Phase Change. I - General Theory, *J. Chem. Phys*., 7[12], 1103-1112 (1939); Kinetics of Phase Change.II - Transformation-Time Relations for Random Distribution of Nuclei, *J. Chem. Phys,* 8[2], 212-224 (1940); Kinetics of Phase Change. III - Granulation, Phase Change, and Microstructure, *J. Chem. Phys,* 9[2], 177–184 (1941).
13. H.J. Borchard, Initial Reaction Rates from DTA, *J. Inorg. Nucl. Chem*., 12, 252–254 (1960).
14. N.P. Bansal and R.H. Doremus, Determination of Reaction Kinetic Parameters from Variable Temperature DSC or DTA, *J. Thermal Anal*., 29, 115 (1984).
15. N.P. Bansal, R.H. Doremus, A.J. Bruce, and C.T. Moynihan, Kinetics of Crystallization of $ZrF_4\text{-}BaF_2\text{-}LaF_3$ Glass by Differential Scanning Calorimetry, *J. Am. Ceram. Soc*., 66 [4], 233 (1983).
16. N.P. Bansal, A. J. Bruce, R.H. Doremus, and C.T. Moynihan, The Influence of Glass Composition on the Crystal Growth Kinetics of Heavy Metal Fluoride Glasses, *J. Non-Cryst. Solids*, 70, 379 (1985).
17. G.O. Piloyan, I.D. Rybachikov, and O.S. Novikova, Determination of Activation Energies of Chemical Reactions by Differential Thermal Analysis, *Nature*, 212, 1229 (1966).
18. N.P. Bansal and M.J. Hyatt, Crystallization Kinetics of Barium Aluminosilicate Glasses, *J. Mater. Res*., 4, 1257 (1989).
19. M.J. Hyatt and N.P. Bansal, Crystal Growth Kinetics in $BaO.Al_2O_3.2SiO_2$ and $SrO.Al_2O_3.2SiO_2$ Glasses, *J. Mater. Sci*., 31 [1], 172–184 (1996).
20. D. Bahadur, N. Lahl, K. Singh, L. Singheiser, and K. Hilpert, Influence of Nucleating Agents on the Chemical Interaction of $MgO\text{-}Al_2O_3\text{-}SiO_2\text{-}B_2O_3$ Glass Sealants with Components of SOFCs, *J. Electrochem. Soc*., 151[4], A558–A562 (2004).

REPORT DOCUMENTATION PAGE

Form Approved
OMB No. 0704-0188

1. AGENCY USE ONLY (*Leave blank*)	2. REPORT DATE	3. REPORT TYPE AND DATES COVERED
	January 2005	Technical Memorandum

4. TITLE AND SUBTITLE

Crystallization Kinetics of a Solid Oxide Fuel Cell Seal Glass by Differential Thermal Analysis

5. FUNDING NUMBERS

WBS–22–066–20–06

6. AUTHOR(S)

Narottam P. Bansal and Eleanor A. Gamble

7. PERFORMING ORGANIZATION NAME(S) AND ADDRESS(ES)

National Aeronautics and Space Administration
John H. Glenn Research Center at Lewis Field
Cleveland, Ohio 44135–3191

8. PERFORMING ORGANIZATION REPORT NUMBER

E–14971

9. SPONSORING/MONITORING AGENCY NAME(S) AND ADDRESS(ES)

National Aeronautics and Space Administration
Washington, DC 20546–0001

10. SPONSORING/MONITORING AGENCY REPORT NUMBER

NASA TM—2005-213436

11. SUPPLEMENTARY NOTES

Prepared for the Ninth International Symposium on Solid Oxide Fuel Cells (SOFC–IX) cosponsored by the Electrochemical Society and the SOFC Society of Japan, Quebec City, Canada, May 15–20, 2005. Narottam P. Bansal and Eleanor A. Gamble (Summer Intern), NASA Glenn Research Center. Responsible person, Narottam P. Bansal, organization code RMC, 216–433–3855.

12a. DISTRIBUTION/AVAILABILITY STATEMENT

Unclassified - Unlimited
Subject Categories: 07 and 27 Distribution: Nonstandard

Available electronically at http://gltrs.grc.nasa.gov

This publication is available from the NASA Center for AeroSpace Information, 301–621–0390.

12b. DISTRIBUTION CODE

13. ABSTRACT ***(Maximum 200 words)***

Crystallization kinetics of a barium calcium aluminosilicate glass (BCAS), a sealant material for planar solid oxide fuel cells, have been investigated by differential thermal analysis (DTA). From variation of DTA peak maximum temperature with heating rate, the activation energy for glass crystallization was calculated to be 259 kJ/mol. Development of crystalline phases on thermal treatments of the glass at various temperatures has been followed by powder x-ray diffraction. Microstructure and chemical composition of the crystalline phases were investigated by scanning electron microscopy and energy dispersive spectroscopic (EDS) analysis. $BaSiO_3$ and hexacelsian ($BaAl_2Si_2O_8$) were the primary crystalline phases whereas monoclinic celsian ($BaAl_2Si_2O_8$) and (Ba_x, Ca_y)SiO_4 were also detected as minor phases. Needle-shaped $BaSiO_3$ crystals are formed first, followed by the formation of other phases at longer times of heat treatments. The glass does not fully crystallize even after long term heat treatments at 750 to 900 °C.

14. SUBJECT TERMS

Solid oxide fuel cells; Seals; Glasses; Crystallization; Devitrification

15. NUMBER OF PAGES

20

16. PRICE CODE

17. SECURITY CLASSIFICATION OF REPORT	18. SECURITY CLASSIFICATION OF THIS PAGE	19. SECURITY CLASSIFICATION OF ABSTRACT	20. LIMITATION OF ABSTRACT
Unclassified	Unclassified	Unclassified	